inter noise
2013 | INNSBRUCK | AUSTRIA
15.-18. SEPTEMBER 2013
NOISE CONTROL FOR QUALITY OF LIFE

Humidity Effect on Pressure-Velocity Sensor Examined in Sound Absorption Measurement with Ensemble Averaging Technique

Toru Otsuru[1], Kusno Asniawaty[2, 3], Reiji Tomiku[3], Takeshi Okuzono[3]
Noriko Okamoto[4], Nazli Bin Che Din[5]

[1] Faculty of Engineering, Oita University, 700 Dannoharu, Oita 870-1192, Japan

[2] Hasanuddin University, Indonesia, [3] Oita University, Japan

[4] Ariake National College of Technology, Japan,

[5] University of Malaya, Malaysia

ABSTRACT

The authors have proposed an absorption measurement method (EA-method) that utilizes ensemble averaging and pressure-velocity sensor (pu- sensor) for measuring surface normal impedance required for wave-based room acoustics simulations. However, through some amount of measurements with pu-sensors, the authors have come to have a question about the effect of humidity to the stability of pu-sensor. Then, employing two pu-sensors with the same specifications, the authors conducted a series of experiment, at four periods from 2010 to 2011. One experiment consists both a pu-sensor calibration and an EA-method measurement. In each calibration or EA-method measurement, relative humidity around pu-sensor was systematically controlled from 35% to 60% with 5% step, and both temperature and atmospheric pressure were monitored. By comparing the standard deviations of resulting absorption coefficients, the authors examined the effect of the relative humidity difference between at the calibration and at the EA-method measurement to resulting absorption coefficient. Final results showed that the standard deviation of absorption coefficient increases as the difference of relative humidity increases. If the difference is kept closer to 0%, the standard deviation of measured absorption coefficient stays smaller.
Keywords: Absorption, Measurement, Particle-velocity sensor

1. INTRODUCTION

The authors have conducted a series of study to investigate the room acoustics by the wave-based computer simulations. [1, 2] To construct the boundary condition of the simulation, surface normal impedances of materials are required. Then, based on the absorption measurement method with two microphone technique given by Allad *et al.*[3], we proposed a method to measure surface normal impedance *in-situ* utilizing ambient noise[4]. Then, we employed a pu-sensor and showed the concept, advantages and practical configurations of our ensemble averaging method (EA-method) both theoretical-computationally and experimentally. [5,6] During the intensive measurements, we built up a hypothesis that atmospheric, especially humidity, fluctuation around the sensor might affect the sensor's stability.[7] Then, the objective of this paper is to verify the hypothesis. A series of

[1] otsuru@oita-u.ac.jp

experiment that consists both of pu-sensor calibration and of EA-method absorption measurement using the pu-sensor was conducted under systematically controlled atmospheric environment and a tendency supporting the hypothesis was obtained.

2. EXPERIMENT METHODOLOGY

2.1 Calibration of Pressure-Velocity Sensor

The absorption measurement by EA-method utilizes the calibration value C_H which is measured in an acoustic tube with the length L. A loudspeaker to radiate an input signal is placed at one end of the tube and the other end is assumed to be hard wall.

A pu-sensor is placed at X m away from the hard wall. By the sensor, particle velocity $u_m(X)$ and sound pressure $p_m(X)$ are measured, and C_H can be defined by

$$C_H = \frac{\rho c \cos\left(k(L-X)\right)}{i \sin\left(k(L-X)\right)} \cdot \frac{u_m(X)}{p_m(X)}, \tag{1}$$

here, i, ρc and k denote imaginary unit, characteristic impedance of air and wave constant, respectively. In the transfer function measurement using the pu-sensor between particle velocity u and sound pressure p, measured transfer function can be calibrated by multiplying the C_H.

2.2 Absorption Measurement by EA-method[5, 6]

The authors introduced surface normal impedance of a material as Eq. (5) considering an ensemble of multiple sound incidences (Fig. 2).

$$Z_{\mathrm{EA}} = \frac{< p >}{< u_{\mathrm{n}} >}. \tag{2}$$

In Eq. (5), $<\ \ >$ and u_{n} respectively denote ensemble average and particle velocity with respect to the normal direction at the material surface; and the impedance is named "ensemble averaged impedance". To check and evaluate the results, "corresponding absorption coefficient" is defined as follows:

$$\alpha_{\mathrm{EA}} = 1 - \left| \frac{Z_{\mathrm{EA}} - \rho c}{Z_{\mathrm{EA}} + \rho c} \right|^2. \tag{3}$$

In a practical measurement, the averaging is performed using a fast Fourier transform (FFT) as

$$Z_{\mathrm{EA}} = \frac{1}{N} \sum^{N} H_{up}, \tag{4}$$

here, H_{up} is the transfer function between u_{n} and p, and N is the averaging number of FFT.

3. EXPERIMENTS

The basic configurations of the experiments, calibration and EA-method measurement, follow the descriptions given in the authors' previous papers[5, 6] except the treatment of humidity control. Likewise, the target frequency of experiments and investigations is from 100 Hz to 1200 Hz.

3.1 Experiment Time and Place

All the experiments were conducted at different four periods, period-1, 2 ,3 and 4. Each period took one or two days, and period-1, 2, 3 and 4 were conducted at December 2010, October 2011, December 2011 and several days after period-3 in December 2011, respectively. All the periods are

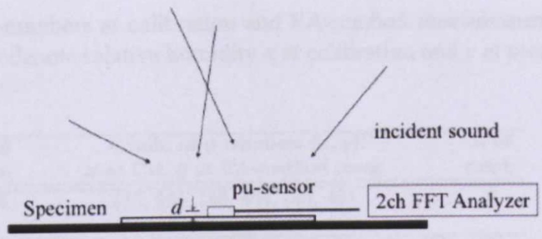

Fig.1 Measurement setup for EA-method. A pu-sensor is located *d* m above a specimen.

at autumn or early winter in southern part of Japan. The general climate was moderate.

All experiments were conducted in a reverberation room of 168 m^3 with non-parallel reinforced concrete walls, located in the basement of Oita University Information Center, a six-street concrete building. Since the reverberation room is acoustically insulated enough from outside environment by double walls with insulating materials, the atmospheric conditions are considerably stable enough to conduct the following experiments.

3.2 Humidity Control

The relative humidity □ inside the reverberation room during the experiment was controlled to a □-number (□ – 35%, 40%, 45%, 50%, 55% and 60%) using a humidifier (Toshiba, KA-N35) and dehumidifiers (Mitsubishi MJ-180EX). To keep uniformity, a conditioning fan was turned on when no experiment was under going.

The atmospheric temperature T_r and □ were measured by thermo-humid meter (CEM DE-321S) with the precision of 0.5◦C and 2% respectively. The atmospheric pressure P was also monitored using a barometer attached to pistonphone (RION NC-72). During all the calibrations and EA-method measurements, T_r, □ and P were monitored at a point 1 m distant from the pu-sensor. The fluctuation ranges of the temperatures and atmospheric pressures at the experiments are 19.6 ◦C ~24.3 ◦C and 1009 hPa~1016 hPa, respectively.

3.3 Calibration Configuration

Using an acoustic tube with L – 0.7 m, two peaces of half inch pu-sensors (Microflown PT0905-32, PT0404-05) with the same specifications were calibrated. Let us call them pu-1 and pu-2, for short. All the calibrations were conducted in the reverberation room, where the relative humidity was controlled at one of the six □-numbers, just before or after the EA-method measurements were conducted in the same room and □-number. Band passed pink noise within 100-1200 Hz was emitted from a loudspeaker (FOSTEX FE-103) at the end of the tube, and the resolution of the 2-channel FFT (RION SA-78) was set to 1.25 Hz employing the Hanning window with 0.8 s time length. Linear averaging of $N = 150$ in the frequency domain with time overlap was performed in 90 s.

3.4 EA-method Configuration

In the reverberation room, where the humidity was controlled at one of the six □-numbers and the calibration was conducted, two EA-method measurements that employed pu-1 and pu-2 successively were conducted using the same FFT with the settings described above. The measured material was a 0.9 m x 0.9 m glass-wool with 32 kg/m^3 density and 50 mm in thickness. The pu-sensor was placed at the center and 0.01 m above of the material. To make the incidence condition closer to random, six loudspeakers (FOSTEX FE-103) mounted in a wooden boxes that radiate incoherent pink noise were placed in the reverberation room. The pink noise was band pass filtered, too. In addition, a sub-woofer (JVC SXDW77) was installed to increase the low-frequency energy, roughly below 200 Hz.

Table 1 Combinations of □-numbers at calibration and EA-method measurement in the □□-cases. The combination (x, y) respectively denote relative humidity x at calibration and y at measurement, which yields □□= | x □y |.

$\Delta\phi$ -case	Comb. of ϕ-numbers (x, y). x at Cal, y at EA-method meas.	n of comb.
0%	(35, 35), (40, 40), (45, 45), (50, 50), (55, 55), (60, 60)	6
5%	(35, 40), (40, 45), (45, 50), (50, 55), (55, 60), (40, 35), (45, 40), (50, 45), (55, 50), (60, 55)	10
10%	(35, 45), (40, 55), (45, 55), (50, 60), (45, 35), (50, 40), (55, 45), (60, 50)	8
15%	(35, 50), (40, 55), (45, 60), (50, 35), (55, 40), (60, 45)	6
20%	(35, 55), (40, 60), (55, 35), (60, 40)	4
25%	(35, 60), (60, 35)	2

3.5 Combination of □-numbers: Calibration and Measurement

All the possible combinations of □-numbers at calibration and at EA-method measurement are listed in Table 1. The following examination process was conducted separately both for pu-1 and pu-2 to confirm the repeatability due to sensor difference.

The examination process for a □□-case is as follows: first, C_H and Z_{EA} were respectively chosen from ξ and η ($\forall\xi, \eta \in \{1, 2, 3, 4\}$). Herein, □□– |x y| stands, and C_H measured at a certain humidity of □– x in a period-ξ was multiplied to Z_{EA} at □= y in a period- η. Thus, calibrated impedance $Z(x, y)_{\xi,\eta}$ and absorption coefficient $\alpha(x, y)_{\xi,\eta}$ were obtained. Next, the moving average in the frequency domain was performed over $Z(x, y)_{\xi,\eta}$ and $\alpha(x, y)_{\xi,\eta}$ to eliminate unnecessary components. Then, to evaluate the stability of the obtained impedance or absorption coefficient, the standard deviation o(□□)$_{\xi,\eta}$ was calculated for each frequency.

4. RESULTS AND DISCUSSION

4.1 Frequency Characteristics of Measured and Calibrated Sound Absorption

Frequency characteristics of processed results of $Z(x, y)_{\xi,\xi}$ and $\alpha(x, y)_{\xi,\xi}$ for □□– 0% and 10% cases calibrated within each one of the four periods (*i.e.*, $\zeta = \eta = 1, 2, 3, 4$) are depicted in Fig. 2. An overall tendency is observed that, as □□ increases, deviations in the three values (real and imaginary parts of impedance, absorption coefficient) increase at each frequency point. Although the other figures are omitted here due to the space limitation, similar tendencies were observed.

Then, the absorption coefficients at the □□= 0% case shown in Fig. 2 were averaged within each period over different combination of □-numbers, and thus calculated mean absorption coefficients □$\alpha(0\%)_{\xi,\xi}$ are compared in Fig. 3 (a) and (b). Furthermore, the absorption coefficients were averaged over both the combination □and measurement period ξ, and resulting mean absorption coefficients □$\alpha(0\%)$ of pu-1 and pu-2 are compared in Fig. 3(c).

In Fig. 3 (a) and (b), the values of □$\alpha(0\%)_{1,1}$ are greater than those of □$\alpha(0\%)_{\xi,\xi}$ of the other periods throughout the frequency range regardless of sensor difference. While, □$\alpha(0\%)_{\xi,\xi}$ of the other periods are close to each other except around 200 Hz. The exceptional behavior of □$\alpha(0\%)_{\xi,\xi}$ can be explained by the diffraction effect from material edges the detail of which have been discussed in our previous paper;[3] and if the averaging is sufficient, the fluctuations can be expected to diminish. Figure 3(c) specifically illustrates that the fluctuations around 200 Hz observed in Figs. 3 (a) and (b) diminish, and that the averaged values of □$\alpha(0\%)_{1,1}$ for pu-1 and pu-2 almost agree each other throughout the frequency range from 100 Hz to 1200 Hz.

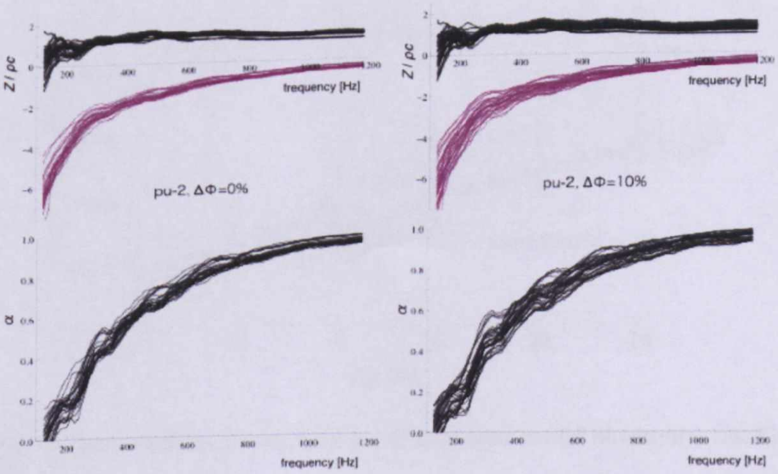

Fig. 3 Frequency characteristics of normalized impedance and sound absorption coefficient measured by pu-2. (left): □□= 0%, (right): □□=10%.

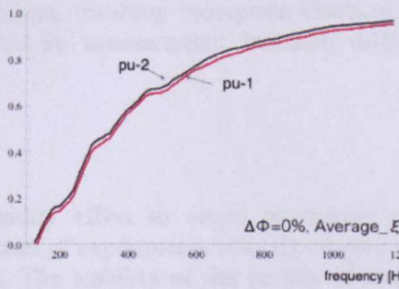

Fig. 4 Comparison of frequency characteristics of averaged sound absorption coefficient between pu-1 and pu-2.

4.2 Humidity Effect onto Standard Deviation of Absorption Coefficient

To concisely compare the difference of deviations in resulting absorption coefficients between different □□cases, the values of standard deviation $\sigma(\square\square)_{\xi,\eta}$ of absorption coefficients were averaged over frequency and the mean values $\bar{\square}(\square\square)_{\xi\eta}$ were obtained both for pu-1 and pu-2.

Thereby, the values are plotted in Fig. 4 comparing the differences between diagonal ($\xi - \eta$) and non-diagonal ($\zeta = \eta$) period-combinations for both the two sensors. The $\bar{\square}(\square\square)_{\xi,\eta}$ values of diagonal period combinations are smaller than those of non-diagonal period-combinations except the □□ – 25% case of pu-2. The differences between the diagonal and non-diagonal period-combinations are less than 0.0063 for pu-1 and 0.0017 for pu-2, and the gradient of pu-1 is larger than that of pu-2 throughout the □□range from 0% to 25%. The differences between diagonal or non-diagonal combinations as well as the different gradients of the lines in Fig. 4 might be attributable to pu-sensor difference.

Irrespective of pu-sensor, however, the increasing tendencies of $\bar{\square}(\square\square)_{\xi\eta}$ with respect to the increase of □□are confirmed quantitatively and repeatedly for all period combinations. Although the absolute value of standard deviation might have no great significance because it depends on the averaging number, the values stay smaller if □□is kept closer to 0%. Diagonal combinations are also preferable than non-diagonal combinations because the former combinations gives smaller standard deviations than latter's except a single □□= 25% case of pu-2.

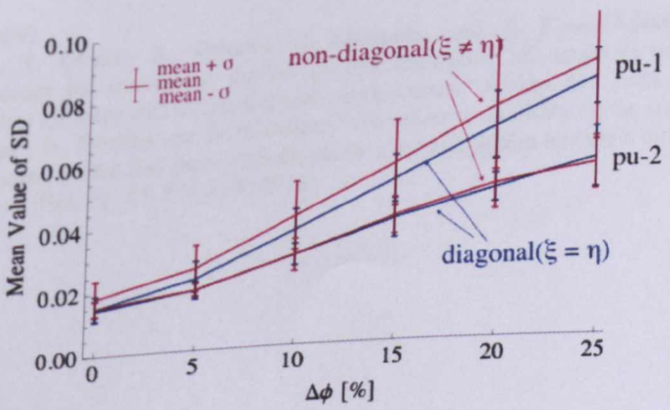

Fig. 4 Comparison of frequency characteristics of averaged sound absorption coefficient between pu-1 and pu-2.

The increasing tendencies of $\bar{\square}$ (□□)$_{\xi,\eta}$ with respect to the increase of □□ are confirmed repeatedly for all the four periods irrespective of pu-sensors. The experiment environments in this paper are limited within such small variation ranges that further investigations are required. However, above investigation implies that if the calibration and measurement are conducted within a short period with stable humidity, temperature and atmospheric pressure, resulting absorption characteristics obtained by a pu-sensor shall have smaller standard deviation. At the measurement, humidity difference □□ can be an indicator of the environment.

5. CONCLUSIONS

The significance of the humidity effect to sound absorption measurements using pu-sensor was quantitatively investigated by a series of experiments with six relative humidity numbers from 35% to 60%, two pu-sensors and four periods. The stability of the results of absorption characteristics measured by pu-sensor is influenced by the relative humidity difference between calibration and measurement. The investigation showed that reliable results with smaller standard deviation of absorption coefficient shall be achieved if the humidity difference is kept closer to 0%. The experiments were carried out in a reverberation room where the other atmospheric conditions were kept considerably stable. Therefore, further confirmations might be necessary. However, above findings assert that a measurement with a pu-sensor is preferable to be calibrated at a time and place closer to those of the measurement, especially when unstable environmental conditions are anticipated, *e.g.* in *in-situ* measurements.

ACKNOWLEDGEMENTS

This work was partly supported by the Grant-in Aid for Scientific Research (B) (24360238) and by the Research Fund at the Discretion of the President, Oita University.

REFERENCES

1. T. Otsuru, T. Sakuma and S. Sakamoto, "Constructing a database of computational methods for environmental acoustics," Acoust. Sci. and Tech., 26 (2), 221-224 (2005).

2. R. Tomiku, T. Otsuru, D. Azuma and Y. Takahashi, "Use of finite element method for comparison of sound field diffuseness in reverberation rooms with and without absorption materials," Acoust. Sci. and Tech., 26 (2), 225-228 (2005).

3. J. F. Allard and Y. Champoux, "*In situ* two-microphone technique for the measurement of the acoustic surface impedance of materials," Noise Control Eng. J. 32, 15-23 (1989).

4. Y. Takahashi, T. Otsuru, and R. Tomiku, "*In situ* measurements of surface impedance and absorption coefficients of porous materials using two microphones and ambient noise," Appl. Acoust., 66, 845-865 (2005).

5. T. Otsuru, N. B. C. Din, R. Tomiku, N. Okamoto, and M. Murakami, "Ensemble averaged surface normal impedance of material using an in-situ technique: Preliminary study using boundary element method," J. Acoust. Soc. Am.,

125, 3784-3791 (2009).
6. N. B. C. Din, T. Otsuru, R. Tomiku, N. Okamoto, and A. Kusno"Measurement method with a pressure-velocity sensor for measuring surface normal impedance of materials using ensemble averaging: Comparison with other methods and its geometrical configuration," Acoust. Sci. Tech., 33, 86-95 (2012).
7. A. Kusno, T. Otsuru, R. Tomiku, and N. Okamoto,"The effect of humidity on the stability of pressure-velocity sensors - A measurement method of absorption characteristics of building materials by using ensemble averaging -" J. Archi. Build. Sci., Vol. 19, 41, 179-184 (2013).